

Monte Carlo simulation of backscattered electrons and energy from thick targets and surface films

Maurizio Dapor

Istituto per la Ricerca Scientifica e Tecnologica (I.R.S.T.), I-38050 Povo, Trento, Italy

(Received 28 January 1992)

Electron-matter interaction is described by a Monte Carlo procedure in which the mean free path is calculated by using a screened Rutherford formula, while energy loss is computed by using the Kanaya and Okayama semiempirical expression. Monte Carlo simulation results of the backscattering coefficient have been compared with the available experimental data. The examined energy range was 5–30 keV, the atomic number range was 4–92, and the tilt angle range was 0° – 80° . The agreement between simulated and experimental data is found to be excellent in the energy range 10–30 keV; also for 5 keV the agreement is very good when the atomic number is lower than 50. Then the mean backscattered energy was computed for bulk targets, unsupported thin films, and surface films.

I. INTRODUCTION

The interaction of an electron beam with a solid target has been studied since the early part of this century.^{1–6} Excellent reviews about this subject have been given by Bothe,⁷ Birkhoff,⁸ and, more recently, Niedrig,⁹ Goldstein *et al.*,¹⁰ Newbury *et al.*,¹¹ and Feldman and Mayer.¹²

Due to the fundamental role played by electron backscattering in scanning electron microscopy, electron probe microanalysis, Auger electron spectroscopy, electron lithography, and radiation damage, since 1960 its calculation became the subject of the work of a number of investigators. Everhart¹³ (large-angle single-elastic-scattering theory) and then Archard¹⁴ (diffusion theory), Body,¹⁵ Tomlin,¹⁶ and Dashen¹⁷ made calculations about the backscattering coefficient r as a function of the atomic number Z in reasonable agreement with the available experimental data. Subsequently Arnal, Verdier, and Vincensini¹⁸ gave a simple expression for r as a function of tilt angle and atomic number. Then primary energy and atomic number dependences of the backscattering coefficient were given by Jacob,¹⁹ Hunger and K uchler,²⁰ Williamson, Antolak, and Meredith,²¹ and Dapor.²² The papers of Kanaya and Okayama,²³ Lantto,^{24,25} Liljequist,²⁶ Iafrate, McAfee, and Ballato,²⁷ Niedrig,⁹ Rogaschewski,²⁸ and Dapor^{29,30} are concerned with the more general theoretical problems of calculating transmission, backscattering, and absorption of electrons impinging on supported and unsupported thin films. On the basis of the Everhart theory, McAfee³¹ obtained a general expression for the energy distribution of the backscattered electrons and Jablonski³² calculated the so-called Auger backscattering factor, a quantity the knowledge of which is of fundamental importance in quantitative Auger electron spectroscopy.³²

Electron-beam solid-target interaction also has been approached by using the so-called Monte Carlo method, a numerical procedure involving random numbers that is able to solve mathematical problems.³³ This method is convenient, for the study of electron penetration in matter, since the probabilistic laws of interaction of an

individual electron with the atoms constituting the target are known. Consequently it is possible to compute the macroscopic characteristics of the interaction processes by simulating a great number of real trajectories and, then, averaging them.³⁴

Leiss, Penner, and Robinson³⁵ proposed Monte Carlo simulations valid for high-energy electrons (5–55 MeV) in carbon. Subsequently Perkins³⁶ proposed a Monte Carlo calculation of transmission and backscattering of 0.4–4.0 MeV electrons penetrating in carbon, aluminium and copper targets. Bishop^{37,38} based his simulations on a screened Rutherford formula (see, for example, Refs. 3, 39, and 40) for the elastic scattering and on the Bethe expression⁶ for calculating energy loss, obtaining the results concerning keV electrons. Similar procedures were subsequently proposed by Murata,⁴¹ Shimizu and co-workers,^{42–44} Love, Cox, and Scott,⁴⁵ and, more recently, by Armigliato *et al.*,⁴⁶ Desalvo, Parisini, and Rosa,⁴⁷ Salvat and Parellada,^{48,49} Newbury *et al.*,¹¹ Joy,⁵⁰ Fitzgerald, Gillies, and Watton,⁵¹ and El Gomati, Ross, and Matthew.⁵² The Ganachaud and Cailler^{53,54} and Ichimura, Shimizu, and Ze-Jun⁵⁵ approaches are based on the partial-wave expansion method (see, for example, Refs. 40, 56, and 57), while the Dapor work^{58,59} is based on the Kanaya and Okayama semiempirical theory.²³ An excellent review of the various Monte Carlo procedures used to describe electron transport in solids has been given by Jablonski.⁶⁰

All the more recent papers show that the Monte Carlo method is a very powerful and reliable procedure to study keV electrons penetrating in matter. The disadvantage of the Monte Carlo methods with respect to the theoretical approaches is the computer time required by computations, because the precision of a numerical simulation depends on the number of calculated trajectories: The rapid evolution of computer calculation capability allow, on the other hand, obtainment of statistically significant results in reasonable computation times.

Also the pseudo-random-number generators available on most compilers are generally quite reliable: a simple way to check the pseudo-random-number generator is to simulate π by generating a lot of pairs of random num-

bers distributed in the range -1 – 1 . If the distribution of the random numbers is uniform then the fraction of generated points which lie within the unit circle should approach $\pi/4$. The pseudo-random-number generator used in the present work, for example, gives a simulated value for π of 3.14 when the number of generated pairs is 10 000.

In the Monte Carlo simulation described here the energy loss has been calculated by using the Kanaya and Okayama semiempirical formula²³ which gives, with respect to the formula of Bethe,⁶ a better agreement with the Cosslett and Thomas experimental data⁶¹ concerning the maximum penetration range (see, for a comparison, Goldstein *et al.*¹⁰). The mean free path has been calculated by using a screened Rutherford formula presuming that only elastic scattering contributes to significant angular deviations.

The Monte Carlo simulation described is used to calculate the backscattering coefficient and the mean backscattered energy for bulk targets at various angles of incidence. The results concerning backscattering coefficients have been compared with the available experimental data,^{20,62–67} and good agreement was found. Then the mean backscattered energy was calculated for supported and unsupported thin films.

II. THEORETICAL REMARKS

In a collision event with an atomic electron or a nucleus, the incident electron both loses energy and changes direction.

Atomic electron excitations or ejections and plasmon excitations affect the energy dissipation and only slightly the electron direction in the solid, while nuclear collisions are nearly elastic and deflect it without relevant kinetic-energy transfer due to the large mass difference between the incident electron and the nucleus.

An electron can lose a large fraction of its energy in a single collision; nevertheless the so-called continuous slowing down approximation is, generally, accepted: In such an approximation the electron is assumed to continuously dissipate its energy during its travel inside the solid. With such an approach we need an equation to express the elastic scattering between electrons and nuclei and another equation to express the rate of energy lost due to the electron-electron collisions.

A. Elastic scattering

In this work the first Born approximation is presumed to be valid during all the electron trajectory followed inside the solid target. We expect, then, that the systematic errors introduced by this approximation on the macroscopic quantities studied (backscattering coefficients and mean backscattered energy) will be more important for the lowest primary energy examined (5 keV). In any case an electron will be considered absorbed when its energy has become lower than the mean ionization energy: In such a way we avoid considering electrons of very low energy for which the partial-wave method is necessary.

We will assume that the penetrating electrons are subject to a screened Coulomb potential $V(r)$ of the form³

$$V(r) = \frac{Ze^2}{r} \exp\left(-\frac{r}{a}\right), \quad (1)$$

where e is the electron charge, Z the target atomic number, and r the distance between the colliding electron and the nucleus. The a parameter in the exponential factor (approximately representing the screening of the nucleus by the orbital electrons) is calculated, as usual, by^{8,9,39}

$$a = \frac{a_0}{Z^{1/3}}, \quad (2)$$

where a_0 is the Bohr radius of hydrogen.

The Born approximation for the described potential gives a differential cross section of the form⁴⁰

$$\frac{d\sigma(\theta)}{d\theta} = \frac{K_n}{E^2} \frac{Z^2 \sin \theta}{(1 - \cos \theta + 2\beta)^2}, \quad (3)$$

where

$$\beta = k \frac{Z^{2/3}}{E}, \quad (4)$$

θ is the scattering angle, $K_n = 3.26 \times 10^{-14}$ (eVcm)², $k = 3.4$ eV, E is expressed in eV and σ in cm².

The elastic mean free path λ can be obtained by integrating the screened Rutherford formula, Eq. (3), in the range 0 – π of θ values

$$\lambda = \frac{1}{N\sigma(\pi)} = \frac{2\beta(1+\beta)E^2}{NK_n Z^2}, \quad (5)$$

where N is the number of atoms per cm³.

The probability $P(\theta)$ of elastic scattering into an angular range from 0 to θ can be calculated as

$$P(\theta) = \frac{\sigma(\theta)}{\sigma(\pi)} = \frac{(1+\beta)(1-\cos\theta)}{(1+2\beta-\cos\theta)}. \quad (6)$$

B. Energy loss

The Kanaya and Okayama semiempirical expression for the energy lost per unit of length $-dE/ds$ is given by²³

$$-\frac{dE}{ds} = \frac{K_e N Z^{8/9}}{E^{2/3}}. \quad (7)$$

If N is expressed in atoms/cm³ and $-dE/ds$ in eV/cm then $K_e = 3.60 \times 10^{-14}$ (eV^{5/3})cm².

From Eq. (7) one obtains

$$s = \int_{E_0}^E \frac{dE}{dE/ds} = \frac{3(E_0^{5/3} - E^{5/3})}{5K_e N Z^{8/9}}, \quad (8)$$

where E_0 is the primary energy and s is the path length corresponding to a mean electron energy E . The maximum penetration range R is the path length corresponding to $E = 0$, namely,

TABLE I. Comparison between the Kanaya and Okayama maximum penetration range and the Cosslett and Thomas experimental data.

Atomic number	Incident energy (keV)	Experimental range (μm)	Kanaya-Okayama range (μm)
13	2.5	0.21	0.13
13	5	0.48	0.41
13	10	1.11	1.31
29	2.5	0.07	0.05
29	5	0.18	0.14
29	10	0.47	0.46
47	2.5	0.06	0.04
47	5	0.14	0.14
47	10	0.39	0.43
47	15	0.81	0.84
79	2.5	0.03	0.03
79	5	0.08	0.08
79	10	0.23	0.27

$$R = \int_{E_0}^0 \frac{dE}{dE/ds} = \frac{3E_0^{5/3}}{5K_e N Z^{8/9}}. \quad (9)$$

In Table I the Kanaya and Okayama maximum penetration range calculated by Eq. (9) is compared with the Cosslett and Thomas experimental data.⁶¹ The agreement is very good.

III. MONTE CARLO SIMULATION

Let us adopt spherical coordinates (r, θ, ϕ) and assume that a stream of monoenergetic electrons irradiates a semi-infinite solid target in the $+z$ direction. The path-length distribution is assumed to follow a Poisson-type law. The step length Δs is then given by^{11,33,42,43,48,59}

$$\Delta s = -\lambda \ln(rnd_1), \quad (10)$$

where rnd_1 is a random number uniformly distributed in the range 0–1 and λ is calculated by using Eq. (5). The energy loss ΔE along the segment of trajectory Δs is approximated by

$$\Delta E = (dE/ds)\Delta s, \quad (11)$$

where dE/ds is computed by using Eq. (7).

The polar scattering angle θ after an elastic collision is calculated assuming that the probability $P(\theta)$ of elastic scattering into an angular range from 0 to θ is a random number rnd_2 uniformly distributed in the range 0–1. By Eq. (6) it follows that

$$\cos \theta = 1 - \frac{2\beta rnd_2}{1 + \beta - rnd_2}. \quad (12)$$

The azimuthal angle ϕ can take on any value in the range 0– 2π selected by a random number rnd_3 uniformly distributed in that range.

Both the θ and ϕ angles are calculated relative to the last direction in which the electron was moving before the

impact. The direction θ'_z in which the electron is moving after the last deflection, relative to the z direction, is given by³⁵

$$\cos \theta'_z = \cos \theta_z \cos \theta + \sin \theta_z \sin \theta \cos \phi, \quad (13)$$

where θ_z is the angle relative to the z direction before the impact. The motion Δz along the z direction is then calculated by

$$\Delta z = \Delta s \cos \theta'_z. \quad (14)$$

The new angle θ'_z then becomes the incident angle θ_z for the next path length.

An electron is followed in its trajectory into the solid target until its energy becomes lower than the mean ionization energy J calculated in eV by⁶⁸

$$J = (9.76 + 58.8Z^{-1.19})Z. \quad (15)$$

The mean energy of the backscattered electrons is simply computed by dividing the sum of their energies by their number. In the present calculation the simulations have been performed on 10 000 trajectories for each primary energy and for each target.

IV. RESULTS AND DISCUSSION

When the electron beam impinges on the solid target, a fraction of the beam is absorbed, another fraction is backscattered, and the remaining fraction is transmitted. The sum of these fractions is equal to 1 and each of them lies in the range 0–1. Their value depends on the target thickness. If the target thickness is greater than the maximum penetration range R no electrons are transmitted through the specimen, the incident electrons can be only absorbed or backscattered, and the fraction of backscattered electrons assumes its maximum value generally indicated as backscattering coefficient. The backscattering coefficient depends on the material, on the electron primary energy, and on the incidence angle.

In Fig. 1 the backscattering coefficient is represented, for various pure elements, as simulated by the described Monte Carlo procedure. The incidence is normal and the examined primary energies range from 5 to 30 keV. A lot of experimental data is available in this energy range.^{20,62–67} They are reported in Fig. 1 to compare the Monte Carlo results with them.

In Fig. 2 the backscattering coefficient dependence on the tilt angle α between the electron direction and normal to the surface is reported for 20-keV electrons and for a number of pure elements. The Monte Carlo results are compared, in this case, with the Neubert and Rogaschewski experimental data.⁶⁷

The agreement between Monte Carlo predictions and experimental data is very good in the energy range 10–30 keV. For 5-keV electrons there is again a satisfactory accordance, at least for the atomic number lower than 50: for $E_0 = 5$ keV and $Z > 50$ departures from experimental results can be observed (less than 20% for the heavier elements, depending on the experimentalist). These departures can be explained by the loss of validity of the

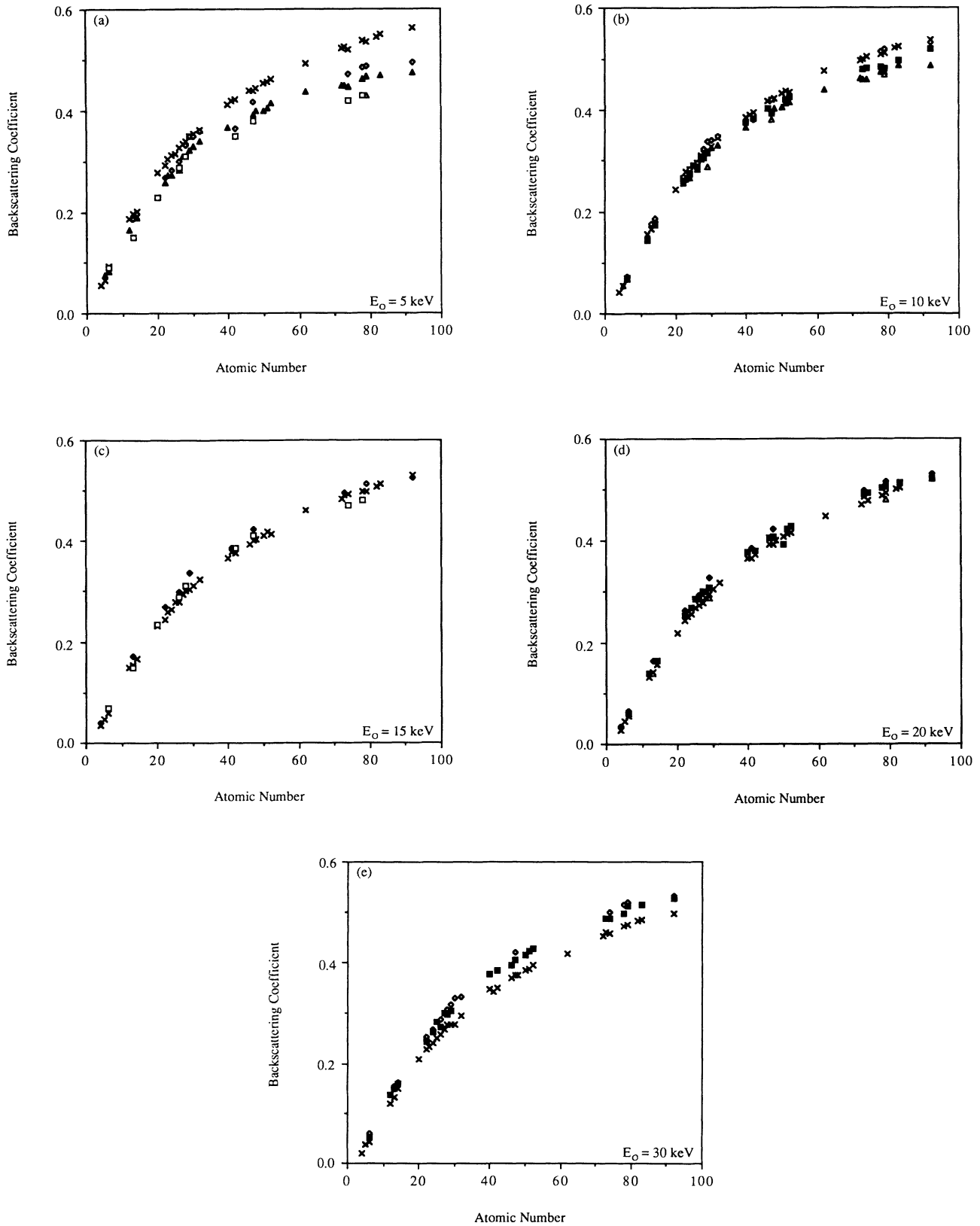


FIG. 1. Backscattering coefficient for various energies and normal incidence as a function of the atomic number (thick targets). (x) Monte Carlo 5 keV (a), 10 keV (b), 15 keV (c), 20 keV (d), and 30 keV (e) simulated data. (\square) 5 keV (a) and 15 keV (c) Palluel; (\triangle) 5 keV (a), 10 keV (b), and 20 keV (d) Cosslett and Thomas; (\diamond) 5 keV (a), 10 keV (b), and 30 keV (e) Bishop; (\blacksquare) 10 keV (b), 20 keV (d), and 30 keV (e) Heinrich; (\blacktriangle) 5 keV (a) and 10 keV (b) Hunger and Kuchler; and (\blacklozenge) 15 keV (c) and 20 keV (d) Neubert and Rogaschewski experimental data.

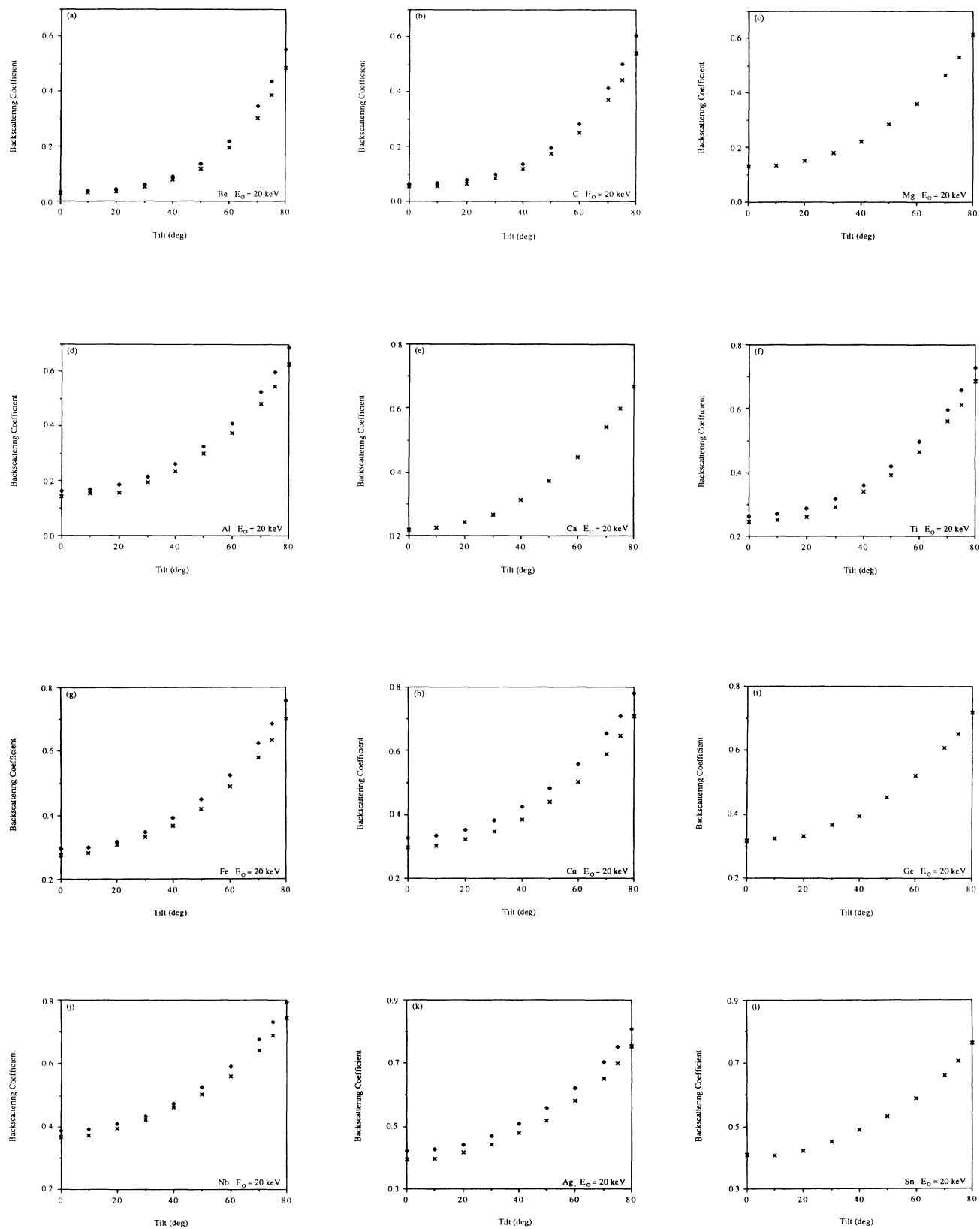


FIG. 2. Backscattering coefficient for various pure elements and 20-keV primary energy as a function of the tilt angle (thick targets). (x) Monte Carlo Be (a), C (b), Mg (c), Al (d), Ca (e), Ti (f), Fe (e), Cu (h), Ge (i), Nb (j), Ag (k), Sn (l), Ta (m), Au (n), Pb (o), and U (p) simulated data. (♦) Neubert and Rogaschewski Be (a), C (b), Al (d), Ti (f), Fe (e), Cu (h), Nb (j), Ag (k), Ta (m), Au (n), and U (p) experimental data.

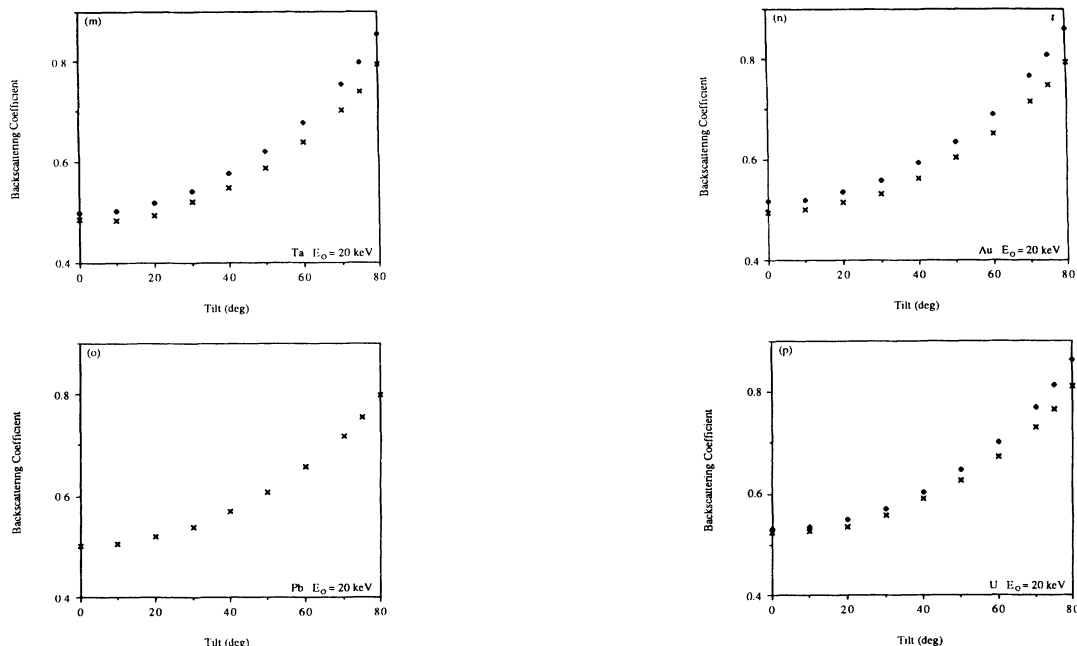


FIG. 2. (Continued).

Born approximation for very low energies and also on the screening parameter used whose dependence on Z , in reality, is not so simple as expressed by Eq. (2).⁹

Let us now consider a surface overlayer, namely a thin film deposited on the top of a substrate constituted of a different material. Compared with the case in which the substrate is not present, the fraction of backscattered electrons is increased, especially for very thin films, due to backscattering from the substrate.^{29,30} In general the backscattered fraction will assume a value between the backscattering coefficient of the substrate and that of a bulk of the material constituting the film, depending on the overlayer thickness.

Curves of backscattering as a function of film thickness for copper, silver, and gold deposited on silicon are presented in Fig. 3 (primary electron energy 20 keV). Similar curves allow the overlayer thickness to be evaluated by simply measuring the backscattering fraction: Obviously this method can be used only when the film atomic number is quite different from that of the substrate.³⁰

Let us now consider the mean backscattered energy. It is not realistic to consider the backscattered electrons as perfectly reflected from the surface without dissipation of energy. It is more reasonable to think that they have penetrated below the surface up to, say, s_B , and have lost a small fraction of their energy. As a consequence the mean energy of the backscattered electrons E_B will be a large fraction of the primary energy whose value will depend on the mean path traveled in the solid before emerging from the surface. Since the mean fractional depth of penetration of backscattered electrons, $u_B = s_B/R$, is increasing as the atomic number decreases,⁶⁴ their energy lost is greater for the light elements with respect to the heavy ones. Therefore the mean energy of backscattered electrons, or its fractional value E_B/E_0 , presented in Fig. 4

for bulk targets and normal incidence, will be an increasing function of the atomic number. Similar trends have been predicted in other papers (see, for example, Refs. 19 and 59).

In Fig. 5 the fractional energy backscattered is presented as a function of the tilt angle α between the electron direction and the normal to the surface, for a number of pure elements: E_B/E_0 increases as α increases and the rate of increase is higher for the lighter elements. As a consequence the variation of the mean backscattered energy is reduced as tilt increases. A similar behavior has

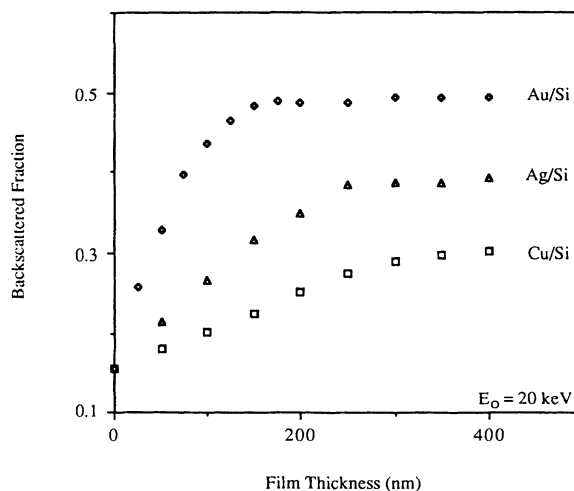


FIG. 3. Fraction of electrons backscattered from surface films deposited on Si for 20-keV electrons and normal incidence as a function of the film thickness. (\square) Cu/Si, (\triangle) Ag/Si, and (\diamond) Au/Si. Simulated data.

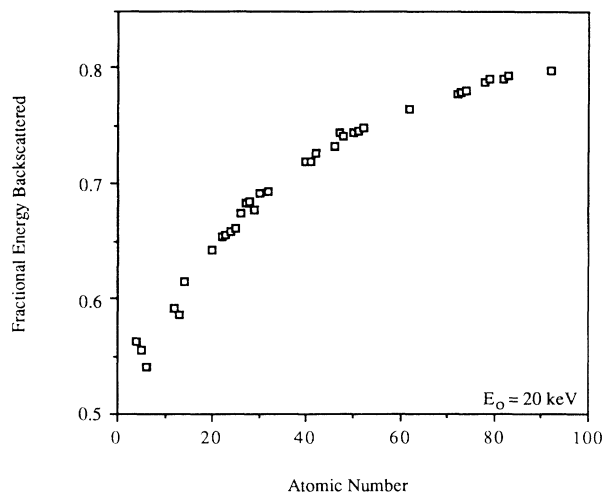


FIG. 4. Fractional energy backscattered from thick targets for 20-keV electrons and normal incidence as a function of the atomic number. Simulated data.

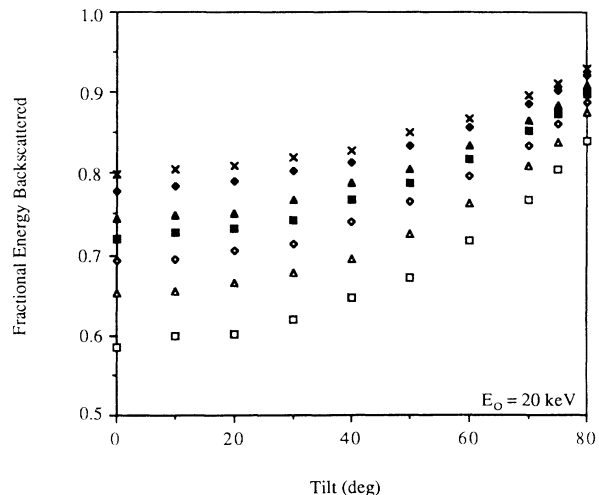


FIG. 5. Fractional energy backscattered from thick targets for 20-keV electrons and various atomic numbers as a function of the tilt angle. (\square) Al, (\triangle) Ti, (\diamond) Ge, (\blacksquare) Nb, (\blacktriangle) Sn, (\blacklozenge) Ta, and (\times) U. Simulated data.

been observed for tilt dependence of the backscattering coefficient⁶⁷ (see Fig. 2).

Up to now we have considered backscattered energy only from bulk targets and we have seen that it is an increasing function both of atomic number and tilt. Let us now consider an unsupported thin film: It is reasonable to think that, for a given material, E_B increases as the film thickness decreases below the mean depth of penetration of backscattered electrons s_B , because electrons can lose less energy inside the solid.

In Fig. 6 we present the fractional energy backscattered from thin films of copper, silver, and gold both unsupported and deposited on silicon. The primary energy examined is 20 keV. The incidence is normal.

The mean depth of penetration of backscattered electrons can be evaluated as the thickness for which the mean backscattered energy from an unsupported thin film becomes constant. With such a definition and calculating the maximum penetration range R by using the Kanaya and Okayama formula [Eq. (9)] we found that the backscattered electrons for copper, silver, and gold come from mean depths equal to $(0.28 \pm 0.02)R$, $(0.22 \pm 0.02)R$

and $(0.18 \pm 0.02)R$, respectively, at 20 keV (see arrows in Fig. 6). On the basis of their experimental data, Cosslett and Thomas gave, for the same quantity, about $0.3R$ for nickel and copper and $0.2R$ for gold, at 25 keV.⁶⁴ As previously observed, the fractional mean depth of penetration of backscattered electrons u_B decreases as the atomic number increases, and, therefore, the mean backscattered energy from thick targets is an increasing function of the atomic number (see Fig. 4).

Let us now consider the curves relative to the supported films. The mean energy backscattered will take on a value influenced both by the presence of the substrate and the film thickness: In particular, if the substrate atomic number is lower than that of the overlayer, a maximum is expected located somewhere before the mean depth of penetration of the backscattered electrons. This is confirmed by the trends presented where, starting from the value of a bulk of silicon, the mean backscattered energy reaches a maximum at about $0.5s_B$ ($0.1R$) and then decreases up to the value corresponding to a bulk of the material constituting the film.

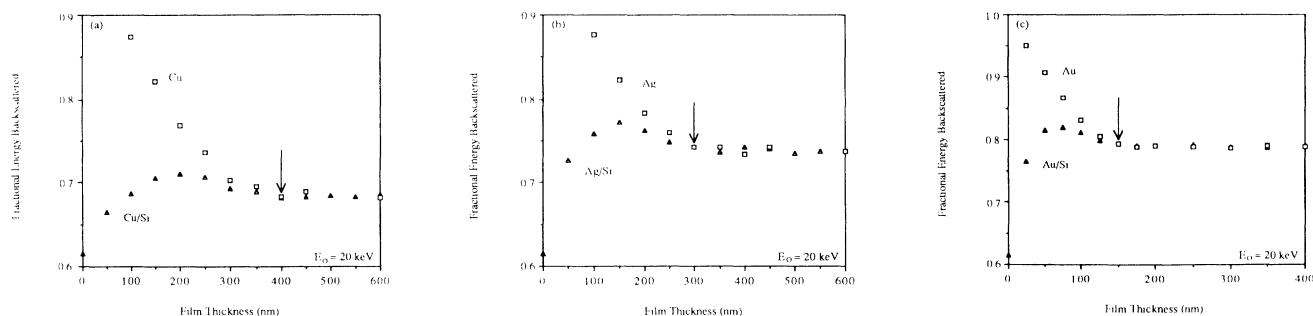


FIG. 6. Fractional energy backscattered from thin films unsupported (\square) and deposited on Si (\triangle) for 20-keV electrons and normal incidence as a function of the film thickness. Cu (a), Ag (b), and Au (c). Arrows indicate the points selected to establish the mean depth of penetration of backscattered electrons. Simulated data.

V. CONCLUSIONS

A Monte Carlo simulation based on a screened Rutherford scattering formula and on the Kanaya and Okayama energy-loss expression has been shown to give results in good agreement with the available experimental data concerning backscattering coefficient in the energy range 5–30 keV.

Then the mean energy backscattered has been com-

puted for thick targets at various angles of incidence and for supported and unsupported thin films. The results have been found to be reasonable and self-contained.

ACKNOWLEDGMENTS

The author wishes to thank Dr. M. Sarkar and Dr. F. Marchetti for frequent and valuable discussions.

- ¹H.W. Schmidt, *Ann. Phys. (Leipzig)* **23**, 671 (1907).
²H.M. Terril, *Phys. Rev.* **22**, 101 (1923).
³G. Wentzel, *Z. Phys.* **40**, 590 (1927).
⁴H. Bethe, *Ann. Phys. (Leipzig)* **87**, 55 (1928).
⁵N.F. Mott, *Proc. R. Soc. London, Ser. A* **124**, 425 (1929).
⁶H. Bethe, *Ann. Phys. (Leipzig)* **5**, 325 (1930).
⁷W. Bothe, in *Handbuch der Physik* (Springer, Berlin, 1933), Vol. 22/2, pp. 1–74.
⁸R.D. Birkhoff, in *Encyclopedia of Physics* (Springer, Berlin, 1958), Vol. 34, pp. 53–138.
⁹H. Niedrig, *J. Appl. Phys.* **53**, R15 (1982).
¹⁰J.I. Goldstein *et al.*, *Scanning Electron and X-Ray Microanalysis* (Plenum, New York, 1984), pp. 53–122.
¹¹D.E. Newbury *et al.*, *Advanced Scanning Electron Microscopy and X-Ray Microanalysis* (Plenum, New York, 1986), pp. 3–43.
¹²L.C. Feldman and J.W. Mayer, *Fundamentals of Surface and Thin Film Analysis* (Elsevier, Amsterdam, 1986), pp. 125–153.
¹³T.E. Everhart, *J. Appl. Phys.* **31**, 1483 (1960).
¹⁴G.D. Archard, *J. Appl. Phys.* **32**, 1505 (1961).
¹⁵Z.T. Body, *Br. J. Appl. Phys.* **13**, 483 (1962).
¹⁶S.G. Tomlin, *Proc. Phys. Soc. London* **82**, 465 (1963).
¹⁷R.F. Dashen, *Phys. Rev.* **134**, A1025 (1964).
¹⁸F. Arnal, P. Verdier, and P.-D. Vincensini, *C. R. Acad. Sci.* **268**, 1526 (1969).
¹⁹J.H. Jacob, *J. Appl. Phys.* **45**, 467 (1974).
²⁰H.J. Hunger and L. K uchler, *Phys. Status Solidi A* **56**, K45 (1979).
²¹W. Williamson, Jr., A.J. Antolak, and R.J. Meredith, *J. Appl. Phys.* **61**, 4612 (1987).
²²M. Dapor, *Phys. Lett. A* **151**, 84 (1990).
²³K. Kanaya and S. Okayama, *J. Phys. D* **5**, 43 (1972).
²⁴V. Lantto, *J. Phys. D* **7**, 703 (1974).
²⁵V. Lantto, *J. Phys. D* **8**, 1341 (1975).
²⁶D. Liljequist, *J. Phys. D* **10**, 1363 (1977).
²⁷G.J. Iafrate, W.S. McAfee, and A. Ballato, *J. Vac. Sci. Technol.* **13**, 843 (1976).
²⁸S. Rogaschewski, *Phys. Status Solidi A* **79**, 149 (1983).
²⁹M. Dapor, *Phys. Rev. B* **43**, 10118 (1991).
³⁰M. Dapor, *Surf. Sci.* (to be published).
³¹W.S. McAfee, *J. Appl. Phys.* **47**, 1179 (1976).
³²A. Jablonski, *Surf. Sci.* **74**, 621 (1978).
³³I.M. Sobol, *The Monte Carlo Method* (MIR, Moscow, 1975), pp. 38–62.
³⁴M.G.C. Cox, in *Quantitative Electron Probe Microanalysis*, edited by V.D. Scott and G. Love (Wiley, Chichester, 1983), pp. 263–282.
³⁵J.E. Leiss, S. Penner, and C.S. Robinson, *Phys. Rev.* **107**, 1544 (1957).
³⁶J.F. Perkins, *Phys. Rev.* **126**, 1781 (1962).
³⁷H.E. Bishop, *Proc. Phys. Soc. London* **85**, 855 (1965).
³⁸H.E. Bishop, *Br. J. Appl. Phys.* **18**, 703 (1967).
³⁹S. Goudsmit and J.L. Sauderson, *Phys. Rev.* **57**, 24 (1940).
⁴⁰J.E.G. Farina, *The International Encyclopedia of Physical Chemistry and Chemical Physics* (Pergamon, Oxford, 1973), Vol. 4.
⁴¹K. Murata, *J. Appl. Phys.* **45**, 4110 (1974).
⁴²R. Shimizu *et al.*, *J. Phys. D* **8**, 820 (1975).
⁴³R. Shimizu *et al.*, *J. Phys. D* **9**, 101 (1976).
⁴⁴R. Shimizu, M. Aratama, S. Ichimura, and Y. Yamazaki, *Appl. Phys. Lett.* **31**, 692 (1977).
⁴⁵G. Love, M.G. Cox, and V.D. Scott, *J. Phys. D* **10**, 7 (1977).
⁴⁶A. Armigliato, A. Desalvo, R. Rinaldi, and R. Rosa, *J. Phys. D* **12**, 1299 (1979).
⁴⁷A. Desalvo, A. Parisini, and R. Rosa, *J. Phys. D* **17**, 2455 (1984).
⁴⁸F. Salvat and J. Parellada, *J. Phys. D* **17**, 185 (1984).
⁴⁹F. Salvat and J. Parellada, *J. Phys. D* **17**, 1545 (1984).
⁵⁰D.C. Joy, *J. Microsc.* **147**, 51 (1987).
⁵¹A.G. Fitzgerald, A.D. Gillies, and H.L.L. Watton, *Surf. Interface Anal.* **16**, 163 (1990).
⁵²M.M. El Gomati, W.C.C. Ross, and J.A.D. Matthew, *Surf. Interface Anal.* **17**, 183 (1991).
⁵³J.P. Ganachaud and M. Cailler, *Surf. Sci.* **83**, 498 (1979).
⁵⁴J.P. Ganachaud and M. Cailler, *Surf. Sci.* **83**, 519 (1979).
⁵⁵S. Ichimura, R. Shimizu, and Ding Ze-Jun, *Surf. Interface Anal.* **13**, 149 (1988).
⁵⁶N.F. Mott and H.S.W. Massey, *The Theory of Atomic Collisions* (Oxford University Press, London, 1965).
⁵⁷E.W. McDaniel, *Atomic Collisions. Electron and Photon Projectiles* (Wiley, New York, 1989).
⁵⁸M. Dapor, *Phys. Lett. A* **143**, 160 (1990).
⁵⁹M. Dapor, *Phys. Lett. A* **158**, 425 (1991).
⁶⁰A. Jablonski, *Surf. Interface Anal.* **14**, 659 (1989).
⁶¹V.E. Cosslett and R.N. Thomas, *Br. J. Appl. Phys.* **15**, 1283 (1964).
⁶²P.C.R. Palluel, *C. R. Acad. Sci.* **224**, 1492 (1947).
⁶³P.C.R. Palluel, *C. R. Acad. Sci.* **224**, 1551 (1947).
⁶⁴V.E. Cosslett and R.N. Thomas, *Br. J. Appl. Phys.* **16**, 779 (1965).
⁶⁵H.E. Bishop, in *Proc. IV Congress internationale optique des rayons x et microanalyse*, edited by R. Castaing, P. Deschamps, and J. Philibert (Hermann, Paris, 1967), pp. 153–158.
⁶⁶K.F.J. Heinrich, in *Proc. IV Congress internationale optique des rayons x et microanalyse* (Ref. 65), pp. 159–167.
⁶⁷G. Neubert and S. Rogaschewski, *Phys. Status Solidi A* **59**, 35 (1980).
⁶⁸M.J. Berger and S.M. Seltzer, National Research Council Publication 1133, Washington D.C., p. 205 (1964).